Journal of
Plankton Research

plankt.oxfordjournals.org

J. Plankton Res. (2016) 38(3): 610–623. First published online April 21, 2016 doi:10.1093/plankt/fbw025

Phylogeography and connectivity of the *Pseudocalanus* (Copepoda: Calanoida) species complex in the eastern North Pacific and the Pacific Arctic Region

JENNIFER MARIE QUESTEL[1]*, LEOCADIO BLANCO-BERCIAL[2], RUSSELL R. HOPCROFT[1] AND ANN BUCKLIN[3]

[1]INSTITUTE OF MARINE SCIENCE, UNIVERSITY OF ALASKA FAIRBANKS, 905 N. KOYUKUK DRIVE, 245 O'NEILL BUILDING, FAIRBANKS, AK 99775, USA, [2]BERMUDA INSTITUTE OF OCEAN SCIENCES–ZOOPLANKTON ECOLOGY, ST. GEORGE'S, BERMUDA AND [3]DEPARTMENT OF MARINE SCIENCES, UNIVERSITY OF CONNECTICUT, 1080 SHENNECOSSETT ROAD, GROTON, CT 06340, USA

*CORRESPONDING AUTHOR: jmquestel@alaska.edu

Received December 14, 2015; accepted March 9, 2016

Corresponding editor: Roger Harris

The genus *Pseudocalanus* (Copepoda, Calanoida) is among the most numerically dominant copepods in eastern North Pacific and Pacific-Arctic waters. We compared population connectivity and phylogeography based on DNA sequence variation for a portion of the mitochondrial cytochrome oxidase I gene for four *Pseudocalanus* species with differing biogeographical ranges within these ocean regions. Genetic analyses were linked to characterization of biological and physical environmental variables for each sampled region. Haplotype diversity was higher for the temperate species (*Pseudocalanus mimus* and *Pseudocalanus newmani*) than for the Arctic species (*Pseudocalanus acuspes* and *Pseudocalanus minutus*). Genetic differentiation among populations at regional scales was observed for all species, except *P. minutus*. The program Migrate-N tested the likelihood of alternative models of directional gene flow between sampled populations in relation to oceanographic features. Model results estimated predominantly northward gene flow from the Gulf of Alaska to the Beaufort Sea for *P. newmani*. Model scenarios that allowed bidirectional gene flow between sampled populations gave the best Bayesian predictions for *P. acuspes*, *P. mimus* and *P. minutus*. Under current warming trends, biogeographical boundaries and barriers for *Pseudocalanus* species may shift, allowing habitat range expansion or contraction and resulting in altered population connectivity between Arctic and sub-Arctic populations.

KEYWORDS: phylogeography; population connectivity; Arctic; zooplankton; *Pseudocalanus*

available online at www.plankt.oxfordjournals.org

INTRODUCTION

Phylogeography studies the patterns of genetic variation within and among species on a geographical scale. Specifically, it incorporates a species' biogeographical past and how underlying forces, such as evolutionary and ecological processes, have structured contemporary geographical distributions (Avise, 2000; Knowles and Maddison, 2002). Portions of mitochondrial genes have frequently been used as genetic markers in phylogeographic studies due to high concentrations of mitochondrial DNA in eukaryotic organisms, its clonal maternal inheritance pattern and the detectable patterns of haplotype diversity within and between populations (Avise, 2000). The mitochondrial cytochrome oxidase I (COI) gene has proven to be a useful genetic marker for studies of marine planktonic copepods to discriminate and identify cryptic species (Bucklin *et al.*, 1998, 2001; Goetze, 2003; Goetze and Ohman, 2010; Viñas *et al.*, 2015), to understand the degree of population connectivity of cosmopolitan species (Goetze, 2005; Blanco-Bercial *et al.*, 2011) and to measure gene flow between distinct geographic populations (Costa *et al.*, 2014). Among other genetic markers used for population genetic and phylogeographic studies of marine copepods are the mitochondrial genes cytochrome B (Provan *et al.*, 2009; Milligan *et al.*, 2011) and 16S rRNA (Goetze, 2003; Nelson *et al.*, 2009), nuclear microsatellites (Provan *et al.*, 2009) and genomic single nucleotide polymorphisms (Brito and Edwards, 2009; Unal and Bucklin, 2010).

In general, holozooplankton are regarded as having very large population sizes and high rates of dispersal, and therefore high evolutionary potential (Peijnenburg and Goetze, 2013). The phylogeographic patterns expressed within holozooplankton populations can be affected by a number of physical mechanisms that create obstructions to gene flow. In addition to physical barriers (Blanco-Bercial *et al.*, 2011), gene flow patterns may be determined by oceanographic features, such as gyre systems (Goetze, 2005) and physical characteristics of the water column including temperature and salinity (Yebra *et al.*, 2011). Temperature and salinity may be the most important structuring factors for the North Pacific Ocean and the Pacific Arctic Region (PAR), which would strongly influence how species' distributions will be altered with continued warming trends. Many zooplankton species are adapted to particular salinity and/or temperature ranges and may see either a range expansion or contraction with projected climate change scenarios. Therefore, it is necessary to understand the hydrographic controls of the study region in order to accurately model and interpret patterns of gene flow within and between zooplankton populations.

Over the past decade, there have been several studies that focused on the population genetics, connectivity and phylogeography of planktonic copepods of the North Pacific and PAR. The sibling species *Calanus glacialis* and *Calanus marshallae*, which present continuing difficulties in identification using morphological characters (Frost, 1974), have been examined using mt16S rRNA, which revealed genetic differences between populations of *C. glacialis* in the North Pacific and Arctic Ocean (Nelson *et al.*, 2009). Studies have provided insights into identification of *Calanus pacificus* subspecies (Nuwer *et al.*, 2008), and evolutionary processes shaping the contemporary phylogeny of the *Neocalanus* genus (Machida *et al.*, 2006).

The copepod genus *Pseudocalanus* is comprised of seven species that co-occur as differing assemblages within their geographic ranges, which span the Arctic and temperate–boreal marine ecosystems of the Northern Hemisphere. They are herbivorous epipelagic filter–feeders that target a wide size range of food particles, such as diatoms, flagellates and coccolithophores (Poulet, 1973; Corkett and Mclaren, 1979; Cleary *et al.*, 2015), and opportunistically feed on sea-ice algae in Arctic regions (Conover *et al.*, 1986). *Pseudocalanus* are small-bodied neritic copepods with *P. newmani* at the smaller end and *P. major* at the larger end of the size spectrum (Frost, 1989). Nonetheless, prosome length alone is not a reliable taxonomic tool for species identification, due to overlapping size ranges and temperature-dependent size shifts. *Pseudocalanus* species display only very subtle morphological differences in the adult stage with diagnostic features dependent upon the shape of the urosomal segment containing the genital pore as well as the shape of the seminal receptacle itself (Frost, 1989). However, species of *Pseudocalanus* show typical levels of interspecific genetic divergence for COI sequences of copepods (10–23%) (Bucklin *et al.*, 2003). These extremely subtle morphological differences have created immense difficulties in accurate species identification and have resulted in a general lack of detailed species-specific distribution data, with co-occurring species typically treated as a species complex and reported simply as *Pseudocalanus* spp.

Pseudocalanus newmani and *Pseudocalanus mimus* are considered as temperate species, while *Pseudocalanus acuspes* and *Pseudocalanus minutus* are Arctic species (Frost, 1989). Within the northern Gulf of Alaska (GoA), the predominant species are *P. mimus* and *P. newmani* with *P. minutus* present in low numbers in both the shelf region and within Prince William Sound (PWS; Napp *et al.*, 2005). *Pseudocalanus mimus* is the most abundant *Pseudocalanus* species in the eastern North Pacific (Napp *et al.*, 2005), and is also found to numerically dominate the outer domains

of the Bering Sea (Bailey *et al.*, 2015). *Pseudocalanus acuspes*, *P. minutus* and *P. newmani* numerically dominate the species complex in the shallow Chukchi (Lane *et al.*, 2008; Hopcroft and Kosobokova, 2010; Hopcroft *et al.*, 2010; Questel *et al.*, 2013) and Beaufort Seas (Horner and Murphy, 1985; Darnis *et al.*, 2008; Smoot, 2015). In the Pacific, the geographical distribution of *P. acuspes* is primarily restricted to the PAR and extends south into the Bering Sea (Bailey *et al.*, 2015), an ecosystem heavily influenced by seasonal ice cover.

Molecular protocols have been developed to discriminate *Pseudocalanus* species based on DNA sequence variation of the COI gene (Bucklin *et al.*, 1995, 2001, 2003), which allows reliable species discrimination and identification. Subsequent studies using this and other genetic markers have allowed researchers to gain better insights into species distribution and abundance (Bucklin *et al.*, 2001, 2015; McGillicuddy & Bucklin, 2002; Grabbert *et al.*, 2010; Bailey *et al.*, 2015; Erikson, 2015), confirmation of presence/absence within a region (Aarbakke *et al.*, 2011; Holmborn *et al.*, 2011), demographic inferences (Aarbakke *et al.*, 2014) and population genetic differentiation (Unal *et al.*, 2006).

This study undertakes a comparative phylogeographic analyses of temperate and Arctic *Pseudocalanus* species and characterizes patterns and pathways of connectivity among populations of four species that are broadly sympatric and numerically dominant in the copepod assemblages of the eastern North Pacific and the PAR (Coyle and Pinchuk, 2003; Llinás *et al.*, 2009; Questel *et al.*, 2013; Ershova *et al.*, 2015). Using COI sequence variation, we infer barriers to gene flow and provide a basis for predicting how the species' geographic distributions and ranges may respond to climate change.

METHOD

Sample collection

Zooplankton samples were collected in 2013 as part of various oceanographic programs conducted in the northern GoA and the PAR (Fig. 1). Samples from the GoA and two fjord systems within PWS (Icy Bay and Columbia Glacier) were collected as part of the Seward Line Research Program (https://www.sfos.uaf.edu/sewardline). Samples from the PAR were collected in the Beaufort Sea during the Transboundary program (Smoot, 2015), and in the Chukchi Sea by the Chukchi Sea Environmental Studies Program (CSESP; Day *et al.*, 2013). All samples were collected down to a maximum of 100 m using 150-μm mesh nets and preserved in 95% nondenatured ethanol following the protocols in Bucklin (2000).

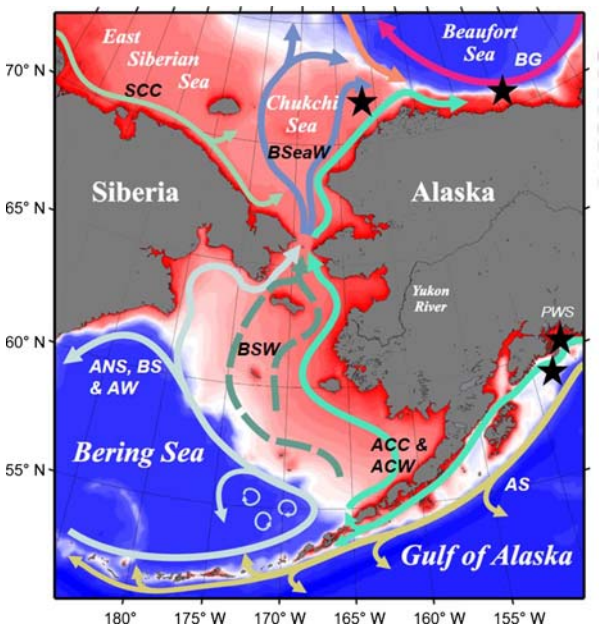

Fig. 1. Averaged current flow fields for the eastern North Pacific Ocean and the PAR. Modified, with consent, from Danielson *et al.* (2011). Stars represent sampling locations. BG, Beaufort Gyre; SCC, Siberian Coastal Current; BSeaW, Bering Sea Water; BSW, Bering Shelf Water; ANS, Aleutian North Slope; BS, Bering Slope; AW, Anadyr Water; ACC, Alaska Coastal Current; ACW, Alaska Coastal Water; AS, Alaskan Stream; PWS, Prince William Sound.

Pathways of transport

The GoA is a semi-enclosed sub-Arctic basin in the North Pacific Ocean that is heavily influenced by the Alaska Coastal Current (ACC), a nutrient-poor, buoyancy-driven current bound to the coastal regions of Alaska (Stabeno *et al.*, 1995, 2004; Weingartner *et al.*, 2005). PWS, a sub-Arctic embayment, is connected to the GoA through two main pathways: Hinchinbrook Entrance on the westernmost side and Montague Strait on the eastern side, through which the ACC enters and exits. The ACC then continues westward through the Aleutian Islands and into the Bering Sea, where it flows along the continental shelf break region (Stabeno *et al.*, 1995). From there, currents flow in a strong northward direction through Bering Strait and across the Chukchi Sea, a shallow shelf ecosystem, in a complicated mixture of water masses (Coachman and Aagard, 1988; Weingartner *et al.*, 1998, 2013). The majority of water flowing over the northeastern Chukchi Sea shelf exits through Barrow Canyon or turns eastward at Point Barrow and flows into the Beaufort Sea (Pickart, 2004). The anticyclonic Beaufort Gyre persists over the Canadian Basin and sets up a countercurrent to the water masses entering the region from the Chukchi Sea. Additionally, water masses situated below the upper

50 m of the water column over the Beaufort Sea's continental slope reverses flow and aids in the transport of Pacific water, and zooplankton, eastward within the Beaufort Undercurrent (Aagaard, 1984; Pickart, 2004). Hence, the dominant northward-flowing currents play an important role in determining the degree of connectivity and the extent of penetration of Pacific copepods into the PAR.

Molecular analysis

Adult female *Pseudocalanus* were picked from preserved zooplankton samples using a Leica MZ16 or M205C dissecting microscope. Key morphological characteristics for species identification, as detailed by Frost (1989), were examined using a compound microscope. Disproportional effort was expended looking for the rarer species within each habitat. Copepods were then washed in sterile MilliQ water to remove traces of ethanol prior to DNA extraction. Total genomic DNA was extracted using a DNeasy Blood and Tissue Kit (QIAGEN), with a final elution volume of 200 µL in AE Buffer.

PCR amplification of a 710-base pair (bp) fragment of the COI gene was achieved using 5 µL of 5 × Green GoTaq® Flexi Buffer, 2.5 µL of 25 mM $MgCl_2$, 0.7 µL of 10 mM dNTPs, 1 µL of each forward and reverse primer (10 µM), 0.15 units of GoTaq® Flexi DNA Polymerase (Promega), 11.8 µL MilliQ water and 3 µL of DNA template, for a total reaction volume of 25 µL. The PCR protocol used was as follows: 94°C for 3 min, 35 cycles of 94°C for 40 s, 60°C for 40 s and 69°C for 50 s, and 1 cycle of 69°C for 7 min. The two primers used were PseudoF: 5′-TTCGAATAGAGYTAGGHMVAGY-3′ (forward) and the Folmer *et al.* (1994) primer HCO-2198: 5′-TAAACTTCAGGGTGACCAAAAAATCA-3′ (reverse). The forward primer, PseudoF, was designed from COI sequences obtained using the primer set LCO-1490 (5′-GGTCAACAAATCATAAAGATATTGG-3′) and HCO-2198 (Folmer *et al.*, 1994).

PCR products were checked by electrophoresis at 100 V for 50 min on a 1% agarose/TBE gel stained with Gel Red (Biotium). Cytochrome oxidase I bands were visualized under a UV light using a UVP ChemiDoc-It^2 imager. PCR products from successful amplifications were purified using 2 µL ExoSAP-IT for every 5 µL PCR product and incubated at 95°C for 15 min.

DNA sequencing used the same primers as for PCR amplification and the Big Dye Terminator Ver. 3.1 kit (Applied Biosystems, Inc., ABI). The cycle sequencing protocol used was modified from Glenn and Schable (2005) and was as follows: 95°C for 1 min, 50 cycles of 96°C for 10 s, 50°C for 5 s and 60°C for 4 min, and 1 cycle of 72°C for 2 min. Sequence reactions were cleaned using the CCDB Sephadex clean-up protocol (www.dnabarcoding.org) and run on an ABI 3130 Genetic Analyzer capillary DNA sequencer. Sequences were manually checked for accurate base calling and contigs generated using the DNA sequence assembly program Sequencher Ver. 5.2.4 (Gene Codes Corp.).

The COI sequences were aligned by CLUSTAL-W (Thompson *et al.*, 1994) using the Molecular Evolutionary Genetics Analysis (MEGA Ver. 6) software package (Tamura *et al.*, 2013). Primers were trimmed from the ends of sequences for an initial aligned length of ~535 bp. Species' identities for COI sequences were verified based on BLAST searches through the NCBI GenBank database (Altschul *et al.*, 1997).

Statistical analysis

Nucleotide diversity (π) and haplotype diversity (H_d) for the COI gene were calculated using the software DnaSP Ver. 5 (Librado and Rozas, 2009). Maximum Parsimony gene trees were analyzed using the best-fit nucleotide substitution model (Tamura model) (Tamura, 1992) as determined by MEGA Ver. 6. The significance of the substitution model was estimated through 10 000 coalescence simulations under a bootstrap test of 1000 replicates. Haplotype networks were determined using Haploviewer (Center for Integrative Bioinformatics; available at http://www.cibiv.at/~%20greg/haploviewer).

A hierarchical Analysis of MOlecular VAriance (AMOVA) was used to examine population genetic structure of each species using the software Arelquin 3.5 (Excoffier and Lischer, 2010). Samples were grouped according to their respective region (i.e. ocean basin; Table I). The significance of the variance partitions, among-regions (Φ_{CT}), among-samples, within-regions (Φ_{SC}) and within-samples (Φ_{ST}), was determined based on 10 100 permutations. F_{ST} distances, reported as Φ_{ST} (Tamura substitution model), were calculated for all pairs of each *Pseudocalanus* species and tested for significance under 10 100 permutations and with $\alpha = 0.05$, after sequential Bonferroni correction (Holm, 1979). Samples with four or fewer individuals were removed from the analysis while all negative Φ_{ST} values obtained were assumed to be zero.

Gene flow between populations of each *Pseudocalanus* species from the GoA, PWS and PAR was modeled using the coalescent-based program Migrate-N Ver. 3.6.11 (Beerli, 2012). Migrate-N uses ratios of maximum likelihood or Bayesian inference to estimate migration rates and effective population size (N_E) under the assumption of asymmetrical migration rates at different subpopulation sizes (Beerli and Felsenstein, 2001; Beerli,

2004, 2006). Custom migration models were constructed for each species of *Pseudocalanus* and structured based on the number of sequences obtained per area, as well as regional geography and hydrography.

For *P. acuspes*, Migrate-N model scenarios tested were as follows: South-to-North, North-to-South and Full (Fig. 2). The South-to-North model tested gene flow from the Chukchi Sea into the Beaufort Sea; the North-to-South scenario tested the reverse flow. The Full model scenario allowed for bidirectional gene flow between both the Chukchi and Beaufort Seas. Model scenarios tested for *P. minutus* and *P. newmani* were: All-North, Part-North, South and Full (Fig. 2). The All-North scenario tested gene flow in a northward flow pattern, with restrictions placed on exchange from more northern populations to southern ones (e.g. Chukchi Sea flowing into the GoA). The Part-North scenario modeled gene flow with unidirectional flow from the GoA into the Chukchi Sea, with bidirectional flow between the Chukchi and Beaufort Seas, as well as between the GoA and PWS populations. The South model was set up to test gene flow from the Beaufort Sea, into the Chukchi Sea and subsequently into the GoA, with bidirectional gene flow between the GoA and PWS populations. The Full model scenario allowed gene flow between all populations, but with restrictions due to geographical constraints. Those restrictions isolated the Beaufort Sea from the GoA and PWS populations, and the Chukchi Sea from the PWS population. Lastly, model scenarios tested for *P. mimus* were: Out-PWS, In-PWS and Full

Table I: Sampling locations and numbers of individuals sequenced for Pseudocalanus *spp. collected during 2013 from the eastern North Pacific and PAR*

Basin	Cruise ID	Station	Bottom depth (m)	Date	Lat (°N)	Long (°W)	*P. acuspes*	*P. minutus*	*P. mimus*	*P. newmani*
Beaufort	TB13	A1-50	50	21 August 2013	70.043	−141.1363	12			
		A2-200	207	19 August 2013	70.512	−142.1004	42	13	1	13
		A2-1000	997	18 August 2013	70.628	−142.2088		2	1	10
		A6-50	50	14 August 2013	70.672	−146.1369	6	3		2
		A6-200	200	14 August 2013	70.889	−146.0859	18	21		8
		A6-1000	1004	17 August 2013	71.014	−146.1102	38	13	1	3
Chukchi	WWW1304	BF007	43	25 September 2013	71.241	−163.4092	39	9	2	9
		KF007	40	21 September 2013	70.772	−165.6299	62	14		9
		KF011	40	23 September 2013	70.895	−166.0141	11	5		4
		KF017	41	22 September 2013	71.021	−165.6390	48	10		8
		SF020	38	30 September 2013	71.994	−164.1493	11			
		TF004	42	3 October 2013	71.247	−164.1828	6			4
PWS	TXF13	CG	193	7 May 2013	60.984	−147.0793	1	28	52	36
		Icy Bay	123	8 May 2013	60.241	−148.3303	1	33	33	63
GoA	TXF13	GAK1	271	5 May 2013	59.841	−149.4697	1	37	17	13
		GAK4	201	5 May 2013	59.402	−149.0572	1		12	13
		GAK8	289	4 May 2013	58.787	−148.4752			10	13
Total							297	188	129	208

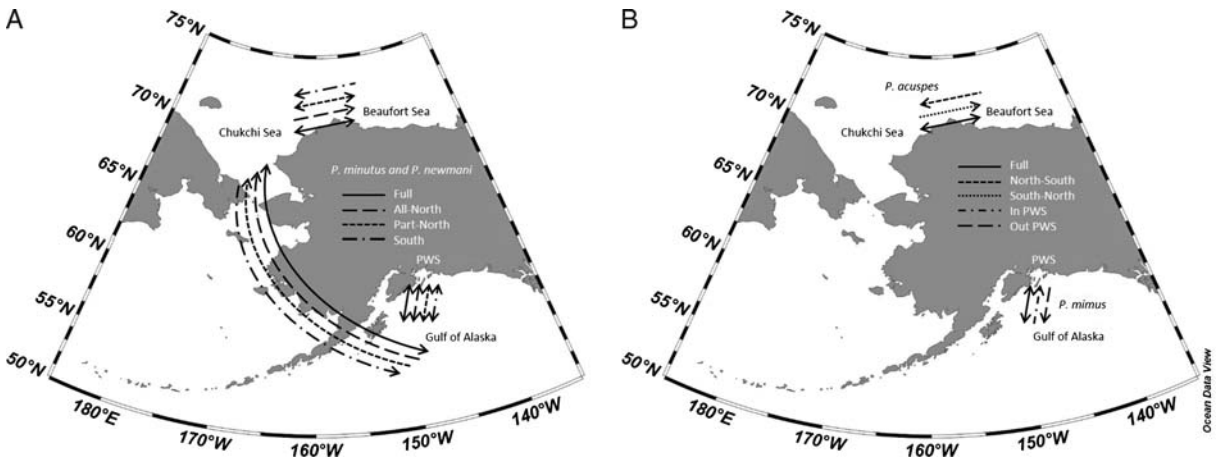

Fig. 2. Conceptual representation of each Migrate-N model scenario tested for *P. minutus* and *P. newmani* (**A**), and *P. acuspes* and *P. mimus* (**B**) in the eastern North Pacific and PAR.

(Fig. 2). The Out-PWS model tested gene flow between Icy Bay and Columbia Glacier—and subsequently out of PWS and into the GoA—whereas the In-PWS model tested gene flow from the GoA into Icy Bay and Columbia Glacier and between the two fjord systems.

Parameters for each Migrate-N model run were kept at the default settings with the following exceptions: (i) parameter start settings for theta (θ) and migration rates (M) used the Mode values from the posterior distributions of an initial run's F_{ST}-based θ and M; (ii) the SLICE sampler method was used for Bayes-proposals for both θ and M and (iii) long-chain values (1–3) were tested for optimal posterior distributions. We report the Bayes factor predictions for custom model scenarios for each species.

RESULTS

A total of 822 COI sequences were obtained for the four *Pseudocalanus* species collected from the GoA, PWS and the Chukchi and Beaufort Seas (Table I; GenBank accession nos KU141424–KU142246). The aligned sequence length used for the analyses ranged from 518 to 536 bp (Table II). *Pseudocalanus minutus* and *P. newmani* were found throughout the entire study region, whereas *P. acuspes* was restricted to the PAR and *P. mimus* was confined to the eastern North Pacific sampling location. Few individuals of *P. acuspes* and *P. mimus* were sequenced from the eastern North Pacific and the PAR, respectively (Table I), despite considerable effort to find them within our collections. The presence of *P. mimus* in the Arctic Ocean has also been confirmed through sequencing the 28S ribosomal RNA gene (GenBank accession no: EF460783).

In all, 178 unique haplotypes were identified among the four species of *Pseudocalanus* over the five sampling regions (Table II). Nucleotide diversity (π) and haplotype diversity (H_d) were lower for the Arctic species *P. acuspes* and *P. minutus* (3.6×10^{-4} and 1.3×10^{-4}; 0.66 and 0.61, respectively), and higher for the temperate species *P. mimus* and *P. newmani* (7.8×10^{-4} and 6.9×10^{-4}; 0.91 and 0.81, respectively; Table II). There were numerous haplotypes for all species, with a range of frequencies for *P. mimus*, and one (in the case of *P. acuspes*) or two (*P. minutus* and *P. newmani*) major haplotypes, with several less frequent or unique haplotypes (Fig. 3). Of the 188 *P. minutus* sequenced, only 13 haplotypes were detected; however, haplotype diversity was almost equal to that expressed for *P. acuspes*. Fifty-two unique haplotypes were identified for *P. mimus*, with only one observed at all five sampling locations, which occurred most frequently (50%) in the Columbia Glacier sample. The two dominant haplotypes for each of *P. minutus* and *P. newmani* were found to be relatively abundant in all five sampling locations, with fairly equal representation exhibited by each haplotype.

Pairwise Φ_{ST} values for samples collected across the four regions showed comparisons between the Chukchi and Beaufort Seas to be significant for *P. acuspes* (Table III). Significant values were also observed for *P. newmani* when Beaufort Sea samples were compared against samples from the GoA and PWS (Table IV). No significant values were observed between samples of *P. minutus* (Table V), while *P. mimus* showed only one significant comparison between one GoA sample and Columbia Glacier (Table VI). Analyses of molecular variance showed significant differentiation of regional populations for *P. acuspes*, *P. mimus* and *P. newmani* (Table VII); no significant differentiation at this scale was found for *P. minutus*. Overall, the greatest amount of variance was explained by individuals within samples for all four species, yet none of the variance components (i.e. variance among regions, among samples within a region or individuals within samples) were statistically significant for *P. minutus*.

Low numbers of *P. acuspes* were found in the GoA and PWS, which constrained the Migrate-N models of gene flow to the PAR. Similarly, low numbers of *P. mimus* were found in the PAR, which constrained the model scenarios of gene flow to the eastern North Pacific. Marginal likelihood outputs predicted the Full model to be the best pathway for gene flow between sampled populations of *P. acuspes* and *P. mimus* (Table VIII). These results indicated strong bidirectional gene flow between the Chukchi and Beaufort Seas for

Table II: Summary of intraspecific variation for COI sequences for Pseudocalanus *from the eastern North Pacific and PAR during 2013*

Affinity	Species	*N*	BP	*H*	π	SD	H_d	SD
Arctic	*P. acuspes*	297	518	59	3.3×10^{-3}	3.6×10^{-4}	0.661	0.032
	P. minutus	188	535	13	1.6×10^{-3}	1.3×10^{-4}	0.606	0.027
Temperate	*P. mimus*	129	536	52	7.8×10^{-3}	4.3×10^{-4}	0.914	0.020
	P. newmani	208	529	54	6.9×10^{-3}	6.6×10^{-4}	0.807	0.020

N, number of individuals sequenced; BP, base pair sequence length; *H*, number of haplotypes; H_d, haplotype diversity; SD, standard deviation; π, nucleotide diversity.

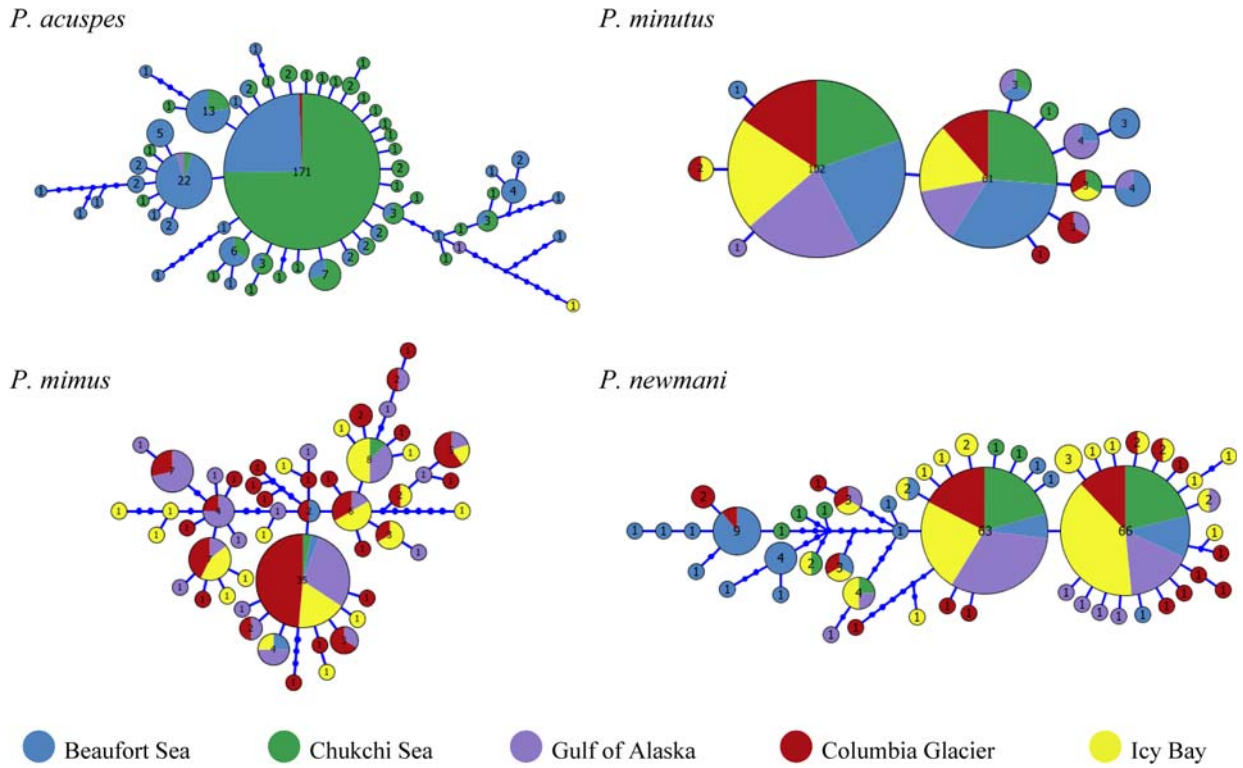

Fig. 3. Cytochrome oxidase I haplotype networks for *P. acuspes*, *P. minutus*, *P. mimus* and *P. newmani*. Each circle represents a unique haplotype; sizes are scaled to the number of individuals expressing that particular haplotype. Each node represents a single bp mutation.

Table III: Pairwise Φ_{ST} distances between samples of P. acuspes *from the eastern North Pacific and PAR during 2013*

P. acuspes	Beaufort Sea					Chukchi Sea					
Samples	A1-50	A2-200	A6-50	A6-200	A6-1000	BF007	KF007	KF011	KF017	SF020	TF004
A1-50		0.215	0.902	0.001	**0.001**	**0.000**	**0.000**	**0.000**	**0.000**	**0.000**	0.061
A2-200	0.016		0.242	0.130	0.008	**0.000**	**0.000**	0.051	**0.000**	0.047	0.264
A6-50	0.000	0.024		0.004	0.017	**0.000**	**0.000**	**0.000**	**0.000**	**0.001**	0.034
A6-200	0.113	0.023	0.199		0.907	0.282	**−0.003**	0.464	0.139	0.336	0.057
A6-1000	**0.168**	0.051	0.247	0.000		0.410	**−0.002**	0.507	0.271	0.323	0.062
BF007	**0.247**	**0.092**	**0.375**	0.004	0.000		0.657	0.580	0.253	0.412	0.007
KF007	**0.310**	**0.127**	**0.414**	**0.024**	**0.013**	0.000		0.377	0.118	0.436	0.007
KF011	**0.142**	0.049	**0.294**	0.000	0.000	0.000	0.005		0.457	1.000	0.096
KF017	**0.249**	**0.105**	**0.343**	0.014	0.005	0.005	0.007	0.000		0.582	0.018
SF020	**0.137**	0.054	**0.305**	0.006	0.000	0.000	0.000	0.000	0.000		0.088
TF004	0.103	0.019	0.220	0.138	0.161	0.290	0.320	0.170	0.236	0.216	

Φ_{ST} values are below and *P* values are above the diagonal. Bold numbers indicate significant values after sequential Bonferroni correction ($\alpha = 0.05$).

P. acuspes and between the GoA and PWS for *P. mimus*. Marginal likelihood outputs predicted the Part-North model, simulating gene flow from the GoA north through the Chukchi Sea and into the Beaufort Sea, to be the best fit for sampled populations of *P. newmani* (Table VIII). All model results for *P. acuspes*, *P. mimus* and *P. newmani* gave good Bayesian unimodal posterior distributions. Marginal likelihood outputs predicted the Full model, which allowed bidirectional gene flow between sampled populations with geographical restrictions, to be the best fit for *P. minutus* (Table VIII). However, Bayesian posterior distributions were not unimodal, but instead showed noisy distributions for all migration rates tested. Models were further tested using Metropolis-Hastings as the Bayes-proposals and longer-running models, with long-chain increments set to 10 000. These parameter changes did not result in cleaner or more unimodal posterior distributions.

Table IV: Pairwise Φ_{ST} distances between samples of P. newmani *from the eastern North Pacific and PAR during 2013*

P. newmani	Beaufort Sea			Chukchi Sea			PWS		GoA		
Stations	A2-200	A2-1000	A6-200	BF007	KF007	KF017	CG	IB	GAK1	GAK4	GAK8
A2-200		0.721	0.079	0.011	**0.001**	0.006	**0.000**	**0.000**	**0.000**	**0.000**	**0.000**
A2-1000	0.000		0.056	0.005	**0.000**	0.004	**0.000**	**0.000**	**0.000**	**0.000**	**0.000**
A6-200	0.140	0.171		0.544	0.287	0.512	0.558	0.013	0.112	0.129	0.116
BF007	0.239	0.296	0.000		0.201	0.574	0.429	0.056	0.345	0.132	0.051
KF007	**0.423**	**0.480**	0.087	0.066		0.900	0.742	0.476	0.668	0.991	0.786
KF017	0.314	0.370	0.000	0.000	0.000		0.926	0.394	0.607	0.761	0.484
CG	**0.347**	**0.393**	0.000	0.000	0.000	0.000		0.061	0.563	0.447	0.436
IB	**0.553**	**0.605**	0.153	0.071	0.000	0.000	0.020		0.970	0.225	0.447
GAK1	**0.449**	**0.508**	0.105	0.028	0.000	0.000	0.000	0.000		0.695	0.698
GAK4	**0.433**	**0.486**	0.097	0.052	0.000	0.000	0.000	0.013	0.000		1.000
GAK8	**0.488**	**0.552**	0.154	0.119	0.000	0.000	0.000	0.000	0.000	0.000	

Φ_{ST} values are below and *P* values are above the diagonal. Bold numbers indicate significant values after sequential Bonferroni correction ($\alpha = 0.05$).

Table V: Pairwise Φ_{ST} distances between samples of P. minutus *from the eastern North Pacific and PAR during 2013*

P. minutus	Beaufort Sea			Chukchi Sea				PWS		GoA
Samples	A2-200	A6-200	A6-1000	BF007	KF007	KF011	KF017	CG	IB	GAK1
A2-200		0.418	0.694	0.614	0.604	0.243	0.747	0.317	0.218	0.736
A6-200	0.000		0.375	0.698	0.292	0.716	0.214	0.101	0.032	0.092
A6-1000	0.000	0.000		0.610	0.833	0.335	0.908	0.801	0.732	0.801
BF007	0.000	0.010	0.000		0.524	0.494	0.614	0.432	0.221	0.435
KF007	0.000	0.000	0.000	0.000		0.212	0.822	0.845	0.740	0.744
KF011	0.041	0.000	0.090	0.000	0.142		0.156	0.146	0.054	0.133
KF017	0.000	0.033	0.000	0.000	0.000	0.156		0.738	0.893	0.733
CG	0.000	0.041	0.000	0.000	0.000	0.111	0.000		0.694	0.506
IB	0.020	0.085	0.000	0.031	0.000	0.228	0.000	0.000		0.449
GAK1	0.000	0.039	0.000	0.000	0.000	0.120	0.000	0.000	0.000	

Table VI: Pairwise Φ_{ST} distances between samples of P. mimus *from the eastern North Pacific and PAR during 2013*

P. mimus	PWS		GoA		
Stations	CG	IB	GAK1	GAK4	GAK8
CG		0.067	**0.001**	0.844	0.856
IB	0.022		0.006	0.553	0.409
GAK1	**0.140**	0.105		0.027	0.017
GAK4	0.000	0.000	0.141		0.978
GAK8	0.000	0.000	0.178	0.000	

Φ_{ST} values are below and *P* values are above the diagonal. Bold numbers indicate significant values after sequential Bonferroni correction ($\alpha = 0.05$).

DISCUSSION

An important component of forecasting how marine ecosystems will respond to climate change is understanding how individual species' distributions and abundances will change with warming trends. Multiyear studies of the mesozooplankton communities from the Chukchi Sea have revealed differing responses on a species level in warm years versus cold years (Matsuno *et al.*, 2011; Questel *et al.*, 2013; Ershova *et al.*, 2015). Specifically, *Pseudocalanus* spp., which numerically dominate the copepod assemblages, are least abundant in colder years (Questel *et al.*, 2013; Ershova *et al.*, 2015). Overall, the temperate *P. newmani* is the most prevalent of the four *Pseudocalanus* species across the Chukchi Sea (Matsuno *et al.*, 2011; Questel *et al.*, 2013; Ershova *et al.*, 2015) exhibiting broader spatial distributions in warmer years and, consequently, pushing faunal barriers for Arctic species northward (Ershova *et al.*, 2015). Interestingly, this exemplifies how even very closely related species, with similar niches and geographical distributions, elicit very different responses to changing environmental conditions.

Results from this study suggest *P. newmani* will likely exhibit greater resilience to climate change, as it was found in high abundances throughout the entire study region and displayed a dominant northward gene flow pattern, concurrent with local hydrography. Conversely, it is plausible that *P. acuspes* will experience, and perhaps

Table VII: Analysis of MOlecular VAriance (AMOVA) for Pseudocalanus *species from the eastern North Pacific and PAR during 2013*

	Source of variation	DF	Sum of squares	Variance components	Percent of variation	Fixation indices	*P* value
Arctic	*P. acuspes*						
	Among regions	1	8.672	**0.0460**	5.45	Φ_{CT} = 0.0545	0.0306 ± 0.0018
	Among samples, within regions	9	15.363	**0.0395**	4.68	Φ_{SC} = 0.0495	0.0008 ± 0.0003
	Within samples	282	213.791	**0.7581**	89.86	Φ_{ST} = 0.1014	0.0000 ± 0.0000
	Total	292	237.826	0.8437			
	P. minutus						
	Among regions	3	1.619	0.0048	1.17	Φ_{CT} = 0.0117	0.2354 ± 0.0038
	Among samples, within regions	6	2.125	−0.0035	−0.85	Φ_{SC} = −0.0086	0.4866 ± 0.0054
	Within samples	174	70.555	0.4055	99.68	Φ_{ST} = 0.0032	0.4172 ± 0.0047
	Total	183	74.299	0.4068			
Temperate	*P. mimus*						
	Among regions	1	3.074	−0.0355	−1.65	Φ_{CT} = −0.0165	0.6045 ± 0.0049
	Among samples, within regions	3	14.349	**0.1245**	5.80	Φ_{SC} = 0.0571	0.0063 ± 0.0008
	Within samples	119	244.690	**2.0562**	95.85	Φ_{ST} = 0.0415	0.0046 ± 0.0006
	Total	123	262.113	2.1453			
	P. newmani						
	Among regions	3	65.476	**0.446**	21.9	Φ_{CT} = 0.2190	0.0210 ± 0.0014
	Among samples, within regions	7	18.015	0.0672	3.30	Φ_{SC} = 0.0423	0.1536 ± 0.0036
	Within samples	184	280.231	**1.5230**	74.79	Φ_{ST} = 0.2521	0.0000 ± 0.0000
	Total	194	363.723	2.0363			

Samples are grouped by region (Chukchi Sea, Beaufort Sea, GoA, Icy Bay and Columbia Glacier). Bold numbers indicate significant values ($P = 0.05$). DF, degrees of freedom.

Table VIII: Bayesian predictions for custom migration models using Migrate-N for Pseudocalanus *from the eastern North Pacific and PAR during 2013*

	P. acuspes	Full	South-to-North	North-to-South	
Arctic	Bezier lmL	**−1841.328**	−1979.752	−1965.854	
	LBF (Besier)	**0.000**	−138.423	−124.526	
	Model Probability	**1.000**	0.000	0.000	
	Choice	**1 (best)**	3	2	
	P. minutus	Full	All-North	Part-North	South
	Bezier lmL	**−972.779**	−983.676	−978.970	−1145.543
	LBF (Besier)	**0.000**	−10.897	−6.190	−172.764
	Model Probability	**0.998**	0.000	0.002	0.000
	Choice	**1 (best)**	3	2	4
	P. mimus	Full	Out-PWS	In-PWS	
Temperate	Bezier lmL	**−1491.687**	−1565.433	−1589.876	
	LBF (Besier)	**0.000**	−73.746	−98.189	
	Model Probability	**1.000**	0.000	0.000	
	Choice	**1 (best)**	2	3	
	P. newmani	Full	All-North	Part-North	South
	Bezier lmL	−1679.050	−1674.089	**−1669.113**	−1806.162
	LBF (Besier)	−9.936	−4.976	**0.000**	−137.048
	Model Probability	0.000	0.007	**0.993**	0.000
	Choice	3	2	**1 (best)**	4

Bold values indicate best model choice.

already has done so, range contraction, where it would be restricted to the colder Arctic environment. *Pseudocalanus acuspes* was very rare in the GoA and PWS regions, being restricted to cold glacial fjords, and thus showed very low levels of population connectivity between the eastern North Pacific and PAR. Overall, results from our Migrate-N model simulations indicate high levels of connectivity between established populations of each *Pseudocalanus* species in the Arctic and eastern North Pacific. Shifting species boundaries will increase the need to understand how climate effects will cascade through marine ecosystems. In particular, northward movement of boreal generalist species has great potential to alter Arctic food webs (Kortsch *et al.*, 2015).

Results from the Migrate-N model scenarios indicated that there is a strong degree of population connectivity between North Pacific and Arctic populations of each of the four species, with bidirectional gene flow occurring between geographically adjacent populations. However, posterior distributions were quite noisy and resolution could not be improved by changing model parameters for *P. minutus*. These results could indicate that either this species has extremely high rates of contemporary gene flow or that it recently went through a population bottleneck, for which single locus mitochondrial data would not be informative enough on their own to definitively model gene flow. In the North Atlantic, *P. minutus* had the lowest level of genetic structuring of the *Pseudocalanus* species studied, with most of the variance explained by within-population comparisons (Aarbakke *et al.*, 2014). Bayesian skyline tests indicated that these populations of *P. minutus* underwent population expansion during the current interglacial 25 000–10 000 YBP (Aarbakke *et al.*, 2014). *Pseudocalanus minutus* was found to be evenly distributed across the Bering Sea, with highest abundances occurring over the shelf region (Bailey *et al.*, 2015). Nucleotide and haplotype diversities expressed within that region were comparable to those found in our study 2.01×10^{-3} and 0.670 (Bailey *et al.*, 2015) versus 1.6×10^{-3} and 0.606, respectively.

Pseudocalanus acuspes appeared to be the most abundant of the four species in the Arctic populations. Despite sharing one highly frequent haplotype, populations of this species showed significant differentiation between the two regions in this study. Our results differ from a prior study, which showed no significant differences among populations (Sevigny *et al.*, 1989). This discrepancy is most likely the result of the reduced ability of allozymes to resolve population structure, as well as analyzing individual *P. acuspes* from a relict population (Bedford Basin) in the North Atlantic that has been genetically isolated since the last glacial maximum. The prospect of a relict population was also observed in the Gulf of Finland, where mitochondrial sequence data revealed a high degree of variance among samples of *P. acuspes*, yet populations exhibited extremely low mitochondrial diversity ($H_d = 0.024$) (Aarbakke *et al.*, 2014), suggesting that these populations started to diverge 200 000–50 000 YBP.

Pseudocalanus mimus and *P. newmani* were found throughout the samples collected from the eastern North Pacific. However, the lack of *P. mimus* within the Chukchi and Beaufort Seas was most likely a result of the abnormally cold temperatures experienced in the PAR for the 2013 open water season (Weingartner *et al.*, 2014), which may have impeded the survival and reproduction of this species on the Bering Sea shelf. Nucleotide and haplotype diversities were high for all populations of *P. mimus* and *P. newmani*, complementing the patterns observed for the Bering Sea populations (Bailey *et al.*, 2015). Aarbakke *et al.* (2014) and Sevigny *et al.* (1989) both observed high levels of sequence diversity for *P. newmani*, with approximations that populations in the North Atlantic have remained stable in size for over 250 000 years (Aarbakke *et al.*, 2014).

Estimates of gene flow for the Full model scenarios for both *P. minutus* and *P. mimus* indicated that population connectivity is bidirectional between the two sampled fjord systems of PWS, as well as within the northern GoA. This flow scenario was also incorporated into the accepted Part-North model for *P. newmani*. These patterns complement the regional hydrographic flow, where the ACC from the GoA enters PWS through Hinchinbrook Entrance and exits through Montague Strait. During the summer months, hydrographic flow decreases in intensity, causing flow to reverse direction (Halverson *et al.*, 2013).

The portion of the Part-North model scenario for *P. newmani* simulating northward gene flow from the GoA through the Chukchi Sea and into to the Beaufort Sea is also consistent with the dominant northward flow of Pacific water through the Bering Sea and across the Chukchi Sea. However, this same model scenario was not the best choice for *P. minutus*. Instead, the model scenario that allowed for southward gene flow from the Chukchi Sea to the GoA gave the best Bayesian predictions. Explanations for these results could be attributed to the periodic southward flow of water through the Bering Strait during the winter months (Woodgate *et al.*, 2005), as well as the low diversity within *P. minutus* populations, which seemingly resulted in multimodal posterior distributions in the Migrate-N model simulations. Therefore, these results should be considered with caution for *P. minutus*. Model scenarios for *P. acuspes*, *P. minutus* and *P. newmani* supported bidirectional gene flow between the Beaufort and Chukchi Seas, which can be accredited to

the juxtaposition of the anticyclonic Beaufort Gyre and the eastward flowing Chukchi Sea water masses setting up a countercurrent flow system in the region.

The moderate levels of haplotype diversity among Arctic species observed in this study may be a direct reflection of population size, where Arctic species have smaller population sizes and ranges than temperate species, thus resulting in lower haplotype diversities. This phenomenon has been observed in other marine copepods (e.g. *Calanus finmarchicus* and *Nannocalanus minor*), which display low mitochondrial diversity and small effective population sizes, most likely resulting from a population contraction during the last glacial maximum (Bucklin and Wiebe, 1998). The low nucleotide diversity, low numbers of alleles over a large number of individuals and moderate H_d recorded for *P. minutus* in this study are likely indications that the evolutionary history of this species entailed genetic isolation or a population bottleneck associated with the closing of the Bering Strait during the Pleistocene Ice Ages (1.6 MYA to 10 000 YBP) due to lower sea level exposing the Bering Land Bridge (Sancetta, 1983).

The phylogeographic analyses presented here confirm the biogeographic distribution of four sibling species of *Pseudocalanus*, which live sympatrically in the eastern North Pacific and PAR (Frost, 1989). Estimates of population connectivity based on COI sequence variation indicated that *Pseudocalanus* species inhabiting the eastern North Pacific and PAR show high levels of gene flow. Similarly, Aarbakke *et al.* (2011) observed a high degree of connectivity among populations of *P. moultoni* in the North Atlantic/Arctic sector. Strong gene flow despite large geographic distances has been observed among the cosmopolitan copepod *Clausocalanus* spp. (Blanco-Bercial *et al.*, 2011) and *Calanus sinicus* (Huang *et al.*, 2014).

Our analyses also revealed gene flow patterns for *P. acuspes*, *P. newmani* and *P. mimus* that agree with local hydrographic flow. For instance, gene flow models indicate a northward flow for populations of *P. newmani* in the GoA through the Chukchi Sea and into the Beaufort Sea, reflecting the dominant northward flow of water masses through the Bering Strait and into the PAR. The temperate species *P. newmani* and the Arctic species *P. minutus* were abundant in all sampling regions, yet genetic structuring was stronger for *P. newmani* compared to *P. minutus*. *Pseudocalanus mimus* (temperate species) and *P. acuspes* (Arctic species) were found in extremely low abundances in Arctic and temperate samples, respectively. These patterns indicate that physical environmental conditions in the eastern North Pacific and PAR, including hydrography and ocean currents, serve as both pathways of exchange and barriers to gene flow for planktonic marine copepods.

ACKNOWLEDGEMENTS

We would like to thank the captains and crews of the *M/V Tiglax*, *R/V Westward Wind* and the *R/V Norseman II* for their help during the various research cruises. In particular, we would like to thank the lead biologists Caryn Rea (ConocoPhilips), Michael Macrander (Shell) and Steinar Eldøy (Statoil) for their contributions to the CSESP project. Sequencing was conducted at the University of Alaska Fairbanks' DNA Core lab facility. We would like to thank the Core Lab director, Ian Herriott, for his continued guidance with laboratory techniques.

FUNDING

This work was primarily supported by the Chukchi Sea Environmental Studies Program (CSESP) funded by ConocoPhillips, Anchorage, AK; Shell Exploration and Production Company, Anchorage, AK and Statoil USA E + P, Inc., Anchorage, AK, with added contributions from UAF through the Northern Gulf of Alaska Applied Research Award. We would also like to thank BOEM for supporting the Transboundary Program as well as NPRB, EVOS and AOOS for supporting the Seward Line cruises, both of which provided samples for this study. Research reported in this publication was supported by an Institutional Development Award (IDeA) from the National Institute of General Medical Sciences of the National Institutes of Health to J.M.Q. (grant number P20GM103395).

REFERENCES

Aagaard, K. (1984) The Beaufort Undercurrent. In Barnes, P. W., Schell, D. M. and Reimnitz, E. (eds.), *The Alaska Beaufort Sea: Ecosystems and Environments*. Academic Press, New York, pp. 47–71.

Aarbakke, O. N. S., Bucklin, A., Halsband, C. and Norrbin, F. (2011) Discovery of *Pseudocalanus moultoni* (Frost, 1989) in Northeast Atlantic waters based on mitochondrial COI sequence variation. *J. Plankton Res.*, **33**, 1487–1495.

Aarbakke, O. N. S., Bucklin, A., Halsband, C. and Norrbin, F. (2014) Comparative phylogeography and demographic history of five sibling species of *Pseudocalanus* (Copepoda: Calanoida) in the North Atlantic Ocean. *J. Exp. Mar. Biol. Ecol.*, **461**, 479–488.

Altschul, S. F., Madden, T. L., Schäffer, A. A., Zhang, J., Zhang, Z., Miller, W. and Lipman, D. J. (1997) Gapped BLAST and PSI-BLAST: a new generation of protein database search programs. *Nucleic Acids Res.*, **25**, 3389–3402.

Avise, J. C. (2000) *Phylogeography: The History and Formation of Species*. Harvard University Press, Cambridge, MA.

Bailey, J., Rynearson, T. and Durbin, E. G. (2015) Species composition and abundance of copepods in the morphologically cryptic genus *Pseudocalanus* in the Bering Sea. *Deep Sea Res. Part II Top. Stud. Oceanogr.* doi:10.1016/j.dsr2.2015.04.017.

Beerli, P. (2004) Effect of unsampled populations on the estimation of population sizes and migration rates between sampled populations. *Mol. Ecol.*, **13**, 827–836.

Beerli, P. (2006) Comparison of Bayesian and maximum-likelihood inference of population genetic parameters. *Bioinformatics*, **22**, 341–345.

Beerli, P. (2012) *Migrate Documentation Version 3.2.1.* Florida State University, Tallahasee, FL, p. 119.

Beerli, P. and Felsenstein, J. (2001) Maximum likelihood estimation of a migration matrix and effective population sizes in n subpopulations by using a coalescent approach. *Proc. Natl Acad. Sci. USA*, **98**, 4563–4568.

Blanco-Bercial, L., Álvarez-Marqués, F. and Bucklin, A. (2011) Comparative phylogeography and connectivity of sibling species of the marine copepod *Clausocalanus* (Calanoida). *J. Exp. Mar. Biol. Ecol.*, **404**, 108–115.

Brito, P. H. and Edwards, S. V. (2009) Multilocus phylogeography and phylogenetics using sequence-based markers. *Genetica*, **135**, 439–455.

Bucklin, A. (2000) Methods for population genetic analysis of zooplankton. In Harris R., Wiebe P., Lenz J., Skjodal H. R. and Huntley M. (eds.), *ICES Zooplankton Methodology Manual.* Academic Press, London, pp. 533–570.

Bucklin, A., Bentley, A. M. and Franzen, S. P. (1998) Distribution and relative abundance of *Pseudocalanus moultoni* and *P. newmani* (Copepoda: Calanoida) on Georges Bank using molecular identification of sibling species. *Mar. Biol.*, **132**, 97–106.

Bucklin, A., Frost, B. W., Bradford-Grieve, J., Allen, L. D. and Copley, N. J. (2003) Molecular systematic and phylogenetic assessment of 34 calanoid copepod species of the Calanidae and Clausocalanidae. *Mar. Biol.*, **142**, 333–343.

Bucklin, A., Frost, B. W. and Kocher, T. D. (1995) Molecular systematics of six *Calanus* and three *Metridia* species (Calanoida: Copepoda). *Mar. Biol.*, **121**, 655–664.

Bucklin, A., Guarnieri, M., Mcgillicuddy, D. J. and Sean Hill, R. (2001) Spring evolution of *Pseudocalanus* spp. abundance on Georges Bank based on molecular discrimination of *P. moultoni* and *P. newmani*. *Deep Sea Res. Part II Top. Stud. Oceanogr.*, **48**, 589–608.

Bucklin, A., Mcgillicuddy, D. J. Jr., Wiebe, P. H. and Davis, C. S. (2015) Habitat usage by the cryptic copepods *Pseudocalanus moultoni* and *P. newmani* on Georges Bank (Northwest Atlantic). *Cont. Shelf Res.*, **111**, 83–94.

Bucklin, A. and Wiebe, P. H. (1998) Low mitochondrial diversity and small effective population sizes of the copepods *Calanus finmarchicus* and *Nannocalanus minor*: possible impact of climatic variation during recent glaciation. *J. Hered.*, **89**, 383–392.

Cleary, A. C., Durbin, E. G., Rynearson, T. A. and Bailey, J. (2015) Feeding by *Pseudocalanus* copepods in the Bering Sea: trophic linkages and a potential mechanism of niche partitioning. *Deep Sea Res. Part II Top. Stud. Oceanogr.* doi:10.1016/j.dsr2.2015.04.001.

Coachman, L. K. and Aagard, K. (1988) Transports through Bering Strait: annual and interannual variability. *J. Geophys. Res.*, **93**, 15515–15539.

Conover, R. J., Herman, A. W., Prinsenberg, S. J. and Harris, L. R. (1986) Distribution of and feeding by the copepod *Pseudocalanus* under fast ice during the arctic spring. *Science*, **232**, 1245–1247.

Corkett, C. J. and Mclaren, I. A. (1979) The biology of *Pseudocalanus*. *Adv. Mar. Biol.*, **15**, 1–231.

Costa, K. G., Filho, L. F. S. R., Costa, R. M., Vallinoto, M., Schneider, H. and Sampaio, I. (2014) Genetic variability of *Acartia tonsa* (Crustacea: Copepoda) on the Brazilian coast. *J. Plankton Res.*, **36**, 1419–1422.

Coyle, K. O. and Pinchuk, A. I. (2003) Annual cycle of zooplankton abundance, biomass and production on the northern Gulf of Alaska shelf, October 1997 through October 2000. *Fish. Oceanogr.*, **12**, 327–338.

Danielson, S., Curchitser, E., Hedstrom, K., Weingartner, T. and Stabeno, P. (2011) On ocean and sea ice modes of variability in the Bering Sea. *J. Geophys. Res.*, **116**, 1–24.

Darnis, G., Barber, D. G. and Fortier, L. (2008) Sea ice and the onshore-offshore gradient in pre-winter zooplankton assemblages in southeastern Beaufort Sea. *J. Mar. Syst.*, **74**, 994–1011.

Day, R. H., Weingartner, T. J., Hopcroft, R. R., Aerts, L. A. M., Blanchard, A. L., Gall, A. E., Gallaway, B. J., Hannay, D. E. *et al.* (2013) The offshore northeastern Chukchi Sea, Alaska: a complex high-latitude ecosystem. *Cont. Shelf Res.*, **67**, 147–165.

Erikson, K. (2015) A time series investigation of the cryptic copepods Pseudocalanus spp. on the NW Atlantic continental shelf. Master's Thesis. University of Connecticut, 48 pp.

Ershova, E. A., Hopcroft, R. R. and Kosobokova, K. N. (2015) Inter-annual variability of summer mesozooplankton communities of the western Chukchi Sea: 2004–2012. *Polar Biol.*, **38**, 1461–1481.

Excoffier, L. and Lischer, H. E. L. (2010) Arlequin suite ver 3.5: a new series of programs to perform population genetics analyses under Linux and Windows. *Mol. Ecol. Resour.*, **10**, 564–567.

Folmer, O., Black, M., Hoeh, W., Lutz, R. and Vrijenhoek, R. (1994) DNA primers for amplification of mitochondrial cytochrome c oxidase subunit I from diverse metazoan invertebrates. *Mol. Mar. Biol. Biotechnol.*, **3**, 294–299.

Frost, B. W. (1974) *Calanus marshallae*, a new species of Calanoid copepod closely allied to the sibling species *C. finmarchicus* and *C. glacialis*. *Mar. Biol.*, **26**, 77–79.

Frost, B. W. (1989) A taxonomy of the marine calanoid copepod genus *Pseudocalanus*. *Can. J. Zool.*, **67**, 525–551.

Glenn, T. and Schable, N. A. (2005) Isolating microsatellite DNA loci. *Methods Enzymol.*, **395**, 202–222.

Goetze, E. (2003) Cryptic speciation on the high seas; global phylogenetics of the copepod family Eucalanidae. *Proc. R. Soc. Lond. B Biol. Sci.*, **270**, 2321–2331.

Goetze, E. (2005) Global population genetic structure and biogeography of the oceanic copepods *Eucalanus hyalinus* and *E. spinifer*. *Evolution*, **59**, 2378–2398.

Goetze, E. and Ohman, M. D. (2010) Integrated molecular and morphological biogeography of the calanoid copepod family Eucalanidae. *Deep Sea Res. Part II Top. Stud. Oceanogr.*, **57**, 2110–2129.

Grabbert, S., Renz, J., Hirche, H. J. and Bucklin, A. (2010) Species-specific PCR discrimination of species of the calanoid copepod *Pseudocalanus*, *P. acuspes* and *P. elongatus*, in the Baltic and North Seas. *Hydrobiologia*, **652**, 289–297.

Halverson, M. J., Bélanger, C. and Gay, S. M. (2013) Seasonal transport variations in the straits connecting Prince William Sound to the Gulf of Alaska. *Cont. Shelf Res.*, **63**, 63–78.

Holm, S. (1979) A simple sequentially rejective multiple test procedure. *Scand. J. Stat.*, **6**, 65–70.

Holmborn, T., Goetze, E., Põllupüü, M. and Põllumäe, A. (2011) Genetic species identification and low genetic diversity in *Pseudocalanus acuspes* of the Baltic Sea. *J. Plankton Res.*, **33**, 507–515.

Hopcroft, R. R. and Kosobokova, K. N. (2010) Distribution and egg production of *Pseudocalanus* species in the Chukchi Sea. *Deep Sea Res. Part II Top. Stud. Oceanogr.*, **57**, 49–56.

Hopcroft, R. R., Kosobokova, K. N. and Pinchuk, A. I. (2010) Zooplankton community patterns in the Chukchi Sea during summer 2004. *Deep Sea Res. Part II Top. Stud. Oceanogr.*, **57**, 27–39.

Horner, R. and Murphy, D. (1985) Species composition and abundance of zooplankton in the nearshore Beaufort Sea in winter-spring. *Arctic*, **38**, 201–209.

Huang, Y., Liu, G. and Chen, X. (2014) Molecular phylogeography and population genetic structure of the planktonic copepod *Calanus sinicus* Brodsky in the coastal waters of China. *Acta Oceanol. Sin.*, **33**, 74–84.

Knowles, L. and Maddison, W. (2002) Statistical phylogeography. *Mol. Ecol.*, **11**, 2623–2635.

Kortsch, S., Primicerio, R., Fossheim, M., Dolgov, A. V., Aschan, M. and Kortsch, S. (2015) Climate change alters the structure of Arctic marine food webs due to poleward shifts of boreal generalists. *Proc. R. Soc. Lond. B Biol. Sci.*, **282**, 1–9.

Lane, P. V. Z., Llinás, L., Smith, S. L. and Pilz, D. (2008) Zooplankton distribution in the western Arctic during summer 2002: hydrographic habitats and implications for food chain dynamics. *J. Mar. Syst.*, **70**, 97–133.

Librado, P. and Rozas, J. (2009) DnaSP v5: a software for comprehensive analysis of DNA polymorphism data. *Bioinformatics*, **25**, 1451–1452.

Llinás, L., Pickart, R. S., Mathis, J. T. and Smith, S. L. (2009) Zooplankton inside an Arctic Ocean cold-core eddy: probable origin and fate. *Deep Sea Res. Part II Top. Stud. Oceanogr.*, **56**, 1290–1304.

Machida, R. J., Miya, M. U., Nishida, M. and Nishida, S. (2006) Molecular phylogeny and evolution of the pelagic copepod genus *Neocalanus* (Crustacea: Copepoda). *Mar. Biol.*, **148**, 1071–1079.

Matsuno, K., Yamaguchi, A., Hirawake, T. and Imai, I. (2011) Year-to-year changes of the mesozooplankton community in the Chukchi Sea during summers of 1991, 1992 and 2007, 2008. *Polar. Biol.*, **34**, 1349–1360.

McGillicuddy, D. J. and Bucklin, A. (2002) Intermingling of two *Pseudocalanus* species on Georges Bank. *J. Mar. Res.*, **60**, 583–604.

Milligan, P. J., Stahl, E. A., Schizas, N. V. and Turner, J. T. (2011) Phylogeography of the copepod *Acartia hudsonica* in estuaries of the northeastern United States. *Hydrobiologia*, **666**, 155–165.

Napp, J. M., Hopcroft, R. R., Baier, C. T. and Clarke, C. (2005) Distribution and species-specific egg production of *Pseudocalanus* in the Gulf of Alaska. *J. Plankton Res.*, **27**, 415–426.

Nelson, R. J., Carmack, E. C., Mclaughlin, F. A. and Cooper, G. A. (2009) Penetration of Pacific zooplankton into the western Arctic Ocean tracked with molecular population genetics. *Mar. Ecol. Prog. Ser.*, **381**, 129–138.

Nuwer, M. L., Frost, B. W. and Armburst, E. V. (2008) Population structure of the planktonic copepod *Calanus pacificus* in the North Pacific Ocean. *Mar. Biol.*, **156**, 107–115.

Peijnenburg, K. T. C. A. and Goetze, E. (2013) High evolutionary potential of marine zooplankton. *Ecol. Evol.*, **3**, 2765–2783.

Pickart, R. S. (2004) Shelfbreak circulation in the Alaskan Beaufort Sea: mean structure and variability. *J. Geophys. Res.*, **109**, C04024.

Poulet, S. A. (1973) Grazing of *Pseudocalanus minutus* on naturally occurring particulate matter. *Limnol. Oceanogr.*, **18**, 564–573.

Provan, J., Beatty, G. E., Keating, S. L., Maggs, C. A. and Savidge, G. (2009) High dispersal potential has maintained long-term population stability in the North Atlantic copepod *Calanus finmarchicus*. *Proc. R. Soc. Lond. B Biol. Sci.*, **276**, 301–307.

Questel, J. M., Clarke, C. and Hopcroft, R. R. (2013) Seasonal and interannual variation in the planktonic communities of the northeastern Chukchi Sea during the summer and early fall. *Cont. Shelf Res.*, **67**, 23–41.

Sancetta, C. (1983) Effect of Pleistocene glaciation upon oceanographic characteristics of the North Pacific Ocean and Bering Sea. *Deep Sea Res.*, **30**, 851–869.

Sevigny, J., Mclaren, I. and Frost, B. (1989) Discrimination among and variation within species of *Pseudocalanus* based on the GPI locus. *Mar. Biol.*, **327**, 321–327.

Smoot, C. A. (2015) Contemporary mesozooplankton communities of the Beaufort Sea. Master's Thesis. University of Alaska Fairbanks, 96 pp.

Stabeno, P. J., Bond, N. A., Hermann, A. J., Kachel, N. B., Mordy, C. W. and Overland, J. E. (2004) Meteorology and oceanography of the Northern Gulf of Alaska. *Cont. Shelf Res.*, **24**, 859–897.

Stabeno, P. J., Reed, R. K. and Schumacher, J. D. (1995) The Alaska Coastal Current: continuity of transport and forcing. *J. Geophys. Res.*, **100**, 2477.

Tamura, K. (1992) Estimation of the number of nucleotide substitutions when there are strong transition-transversion and G+C-content biases. *Mol. Biol. Evol.*, **9**, 678–687.

Tamura, K., Stecher, G., Peterson, D., Filipski, A. and Kumar, S. (2013) MEGA6: molecular evolutionary genetics analysis version 6.0. *Mol. Biol. Evol.*, **30**, 2725–2729.

Thompson, J. D., Higgins, D. G. and Gibson, T. J. (1994) CLUSTAL W: improving the sensitivity of progressive multiple sequence alignment through sequence weighting, position-specific gap penalties and weight matrix choice. *Nucleic Acids Res.*, **22**, 4673–4680.

Unal, E. and Bucklin, A. (2010) Basin-scale population genetic structure of the planktonic copepod *Calanus finmarchicus* in the North Atlantic Ocean. *Prog. Oceanogr.*, **87**, 175–185.

Unal, E., Frost, B. W., Armbrust, V. and Kideys, A. E. (2006) Phylogeography of *Calanus helgolandicus* and the Black Sea copepod *Calanus euxinus*, with notes on *Pseudocalanus elongatus* (Copepoda, Calanoida). *Deep Sea Res. Part II Top. Stud. Oceanogr.*, **53**, 1961–1975.

Viñas, M. D., Blanco-Bercial, L., Bucklin, A., Verheye, H., Bersano, J. G. F. and Ceballos, S. (2015) Phylogeography of the copepod *Calanoides carinatus s.l.* (Krøyer) reveals cryptic species and delimits *C. carinatus s.s.* distribution in SW Atlantic Ocean. *J. Exp. Mar. Biol. Ecol.*, **468**, 97–104.

Weingartner, T. J., Cavalieri, D. J., Aagaard, K. and Sasaki, Y. (1998) Circulation, dense water formation, and outflow on the northeast Chukchi Shelf. *J. Geophys. Res.*, **103**, 7647.

Weingartner, T. J., Danielson, S. L. and Royer, T. C. (2005) Freshwater variability and predictability in the Alaska Coastal Current. *Deep Sea Res. Part II Top. Stud. Oceanogr.*, **52**, 169–191.

Weingartner, T. J., Dobbins, E., Danielson, S., Winsor, P., Potter, R. and Statscewich, H. (2013) Hydrographic variability over the

northeastern Chukchi Sea shelf in summer-fall 2008–2010. *Cont. Shelf Res.*, **67**, 5–22.

Weingartner, T. J., Danielson, S., Dobbins, E. and Potter, R. (2014) *Physical Oceanographic Measurements in the Northeastern Chukchi Sea: 2013*. University of Alaska Fairbanks, Fairbanks, AK, p. 64.

Woodgate, R. A., Aagaard, K. and Weingartner, T. J. (2005) A year in the physical oceanography of the Chukchi Sea: moored measurements from autumn 1990–1991. *Deep Sea Res. Part II Top. Stud. Oceanogr.*, **52**, 3116–3149.

Yebra, L., Bonnet, D., Harris, R. P., Lindeque, P. K. and Peijnenburg, K. T. C. A. (2011) Barriers in the pelagic: population structuring of *Calanus helgolandicus* and *C. euxinus* in European waters. *Mar. Ecol. Prog. Ser.*, **428**, 135–149.